

WIDEBAND CHANNEL MEASUREMENTS AND CHARACTERISATION FOR BROADBAND WIRELESS ACCESS

C L Hong¹, I J Wassell¹, G E Athanasiadou¹, S Greaves² and M Sellars²

¹University of Cambridge, UK

²Cambridge Broadband Limited, UK

Introduction

The fundamental limit that is imposed on any wireless system is due to the radio channel. Propagation and channel models are essential for the analysis and simulation of wireless systems. Knowledge of the radio channel is essential to the development and deployment of a wireless system. Radio channel models are used to support research into methods for mitigating channel impairments, such as the design of the equaliser and the choice of single-carrier or multi-carrier systems (1). In addition, they also form an integral part of wireless system planning and deployment.

There is a large body of literature concerning the mobile radio channel, but literature on the Fixed Wireless Access (FWA) channel is still very limited, mainly due to the fact that it is a relatively new technology compared with mobile radio. In FWA, the Subscriber Unit (SU) is normally installed under-the-eaves/window of a building or at rooftop height (4 – 10 m height) using a directional antenna. In comparison, the height of the receiver antenna in mobile wireless access (MWA) would normally be at street level (1-2m) and its antenna pattern is nominally omnidirectional. These differences together with the higher frequency range (3.5 GHz in FWA c.f. 1-2 GHz in MWA) render the propagation models widely used in MWA unsuitable for use in FWA.

Previous works have investigated the narrowband channel characteristics of FWA systems, also commonly known as wireless local loop, e.g. Crosby et al (2). As the data rate of FWA systems increases, the effect of the wideband channel plays an increasingly important role on system performance. It is therefore necessary to characterise the wideband channel effects. Investigation into the effects of Wideband channels on FWA systems have been conducted in the 2.5 GHz frequency band by Porter et al (3) and Gans et al (4), at 1.9 GHz frequency band by Erceg et al (5); and at the 3.5 GHz by Siaud et al (6). It has been reported that the directional subscriber antennas usually employed in FWA systems significantly reduce the delay spread of the channel compared with that when an omnidirectional antenna is used. However the influence of antenna height has not previously been thoroughly investigated.

This paper presents the results of propagation measurements at 3.5 GHz for a Broadband Fixed

Wireless Access (BFWA) system with a directional subscriber antenna and a sectored base station antenna. First we describe the equipment and data processing methods used for extracting the channel impulse response. This is followed by the results of narrowband path loss measurements, and the statistics of the Root Mean Squared (RMS) delay spread, with respect to SU antenna height.

Measurement Methods

The measurements were conducted in the northern suburbs of Cambridge, during the summer months from June to September 2002 with trees in full foliage. This area has a relatively flat terrain and few high rise buildings, and covers an area of 9 km². The base station (BS) is located at a height of 15 m above ground level. The SU antenna is positioned on top of a retractable vehicle mounted mast. Two sets of readings are taken at each location separated by about 2m. At each location, the bearing of the antenna is adjusted to point in the direction with highest received power. Then the height of the SU antenna is varied between 4 to 10 m in steps of 1 m. At each height, a total of 100 delay profiles and path loss measurement were collected over a period of 30 seconds. A total of 540 sets of measurement have been collected, from 65 subscriber locations with BS to SU distances ranging from 730 m to 3.1 km. The precise locations of the measurement sites are identified with a GPS receiver.

The BS antenna and the SU antenna have half power beamwidths of 90° and 20° respectively, and are both vertically polarised. The gains of the BS and SU antennas are 12.5dBi and 15.6dBi respectively. The bandwidth of the system is 5 MHz, giving rise to delay spread resolution of 200 ns. The length of the pseudo-random sounding sequence is 128 symbols. The sounding sequence is modulated using QPSK. At the subscriber, the received sounding burst is captured on the hard disk of a computer for later processing. A post-processing method based on correlation processing extracts the power delay profiles and the RMS delay spread from the stored data.

Data Processing Methods

The radio channel is often modelled as a linear time-variant filter with impulse response $h(t, \tau)$ or

equivalently by its frequency response $H(f,t)$, where $h(t, \tau)$ and $H(f,t)$ are a Fourier transform pair, Bello (7). Without loss of generality, consider a linear time-invariant system that is characterised by its impulse response $h(\tau)$, as shown in Figure 1.

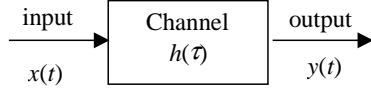


Figure 1. Linear single input/single output system

The complex envelope of the channel output $y(t)$ is the convolution of the impulse response $h(\tau)$ with the complex envelope of the channel input $x(t)$, i.e.

$$y(t) = x(t) \otimes h(\tau) = \int_{-\infty}^{\infty} h(\tau)x(t-\tau)d\tau \quad (1)$$

The time-invariant impulse response $h(\tau)$ is a special case of the time-variant impulse response $h(t, \tau)$ if the unit impulse response function is independent of the time an input is applied, i.e.,

$$h(t, \tau) = h(\tau) \quad \text{for } -\infty < t < \infty \quad (2)$$

To estimate the channel impulse response $h(\tau)$, the first step is to cross-correlate the input of the channel with its output, assuming that the input to the channel, i.e. the transmitted signal, is known. For jointly stationary stochastic processes $x(t)$ and $y(t)$, it can be shown (Proakis (8)) that their cross-correlation $\phi_{xy}(\tau)$ is related to the autocorrelation of the input $\phi_{xx}(\tau)$ as

$$\phi_{xy}(\tau) = \int_{-\infty}^{\infty} h(\alpha)\phi_{xx}(\tau-\alpha)d\alpha \quad (3)$$

which is a convolution integral. Since convolution in time domain is equivalent to multiplication in frequency domain, the relation (3) becomes

$$\Phi_{xy}(f) = \Phi_{xx}(f)H(f) \quad (4)$$

where $\Phi_{xy}(f)$ denotes the Fourier transform of $\phi_{xy}(\tau)$, $\Phi_{xx}(f)$ denotes the Fourier transform of $\phi_{xx}(\tau)$ and $H(f)$ is the frequency response of the channel. Hence, the channel impulse response $h(\tau)$ is found via the inverse Fourier transform of its frequency response $H(f)$. This forms the basis of the technique used in the post-processing algorithm.

The power delay profile is the expected value of the magnitude squared of $h(\tau)$, i.e.,

$$P(\tau) = \frac{E[|h(\tau)|^2]}{2} \quad (5)$$

The RMS delay spread of the channel is calculated according to

$$\tau_{RMS} = \sqrt{\frac{1}{P_T} \sum_{i=1}^n P_i \tau_i^2 - \tau_0^2} \quad (6)$$

where

$$\tau_0 = \frac{1}{P_T} \sum_{i=1}^n P_i \tau_i \quad (7)$$

A Blackman window is applied to the signals before Discrete Fourier transformation. This enhances the signal to noise ratio of the power delay profile to more than 30dB. Since RMS delay spread is known to be sensitive to noise components on the power delay profile having large excess delays (Cullen (9)), a noise exclusion threshold is applied on the power delay profile so that any components more than 30dB below the peak response are excluded before calculating the RMS delay spread. Using this criteria, 432 sets of measurements out of a total of 540 sets were processed and the results are presented as follows.

Results

Figure 2 shows the frequency response of a channel with severe frequency selective fading. The corresponding power delay profile (Figure 3) shows strong time dispersion. The average delay profile plotted in Figure 4 shows a strong echo some 20dB below and delayed by 9 symbol periods (180 ns) from the main peak.

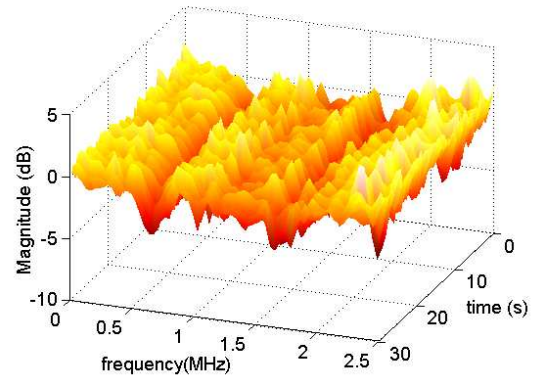


Figure 2. Sample frequency response of a channel

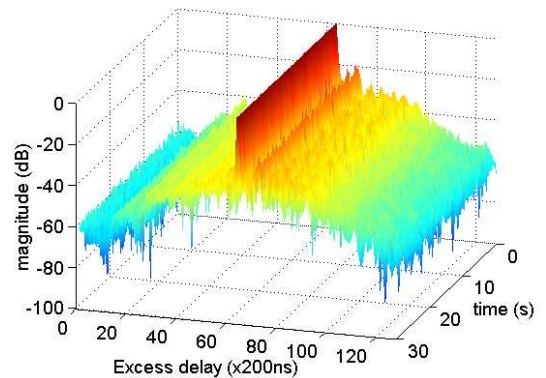


Figure 3. Sample power delay profile of a channel

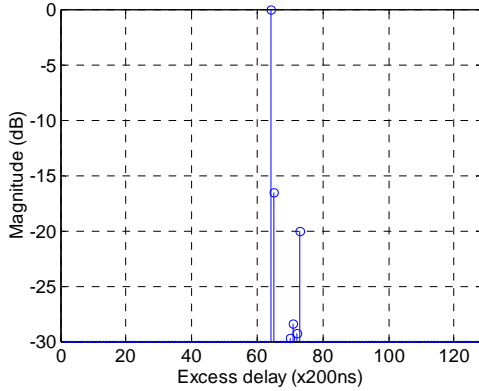


Figure 4. Average power delay profile of the sample channel with noise removed

The RMS delay spread of this channel is 196 ns, and it is one of the worst channels encountered. The SU in this case is located at 0.74 km from the BS at a height of 7.2m above ground.

Path Loss Results

The path loss as a function of the distance between BS to SU for SU antenna heights of 6m, 7m, 8m, 9m, 10m above ground level are plotted in Figure 5. The path loss versus distance is not plotted for a height of 5m above ground level owing to insufficient data. The least-square regressions fits to the data are also plotted for each SU antenna height. The equation of the regression analysis takes the form of

$$PL(d)(dB) = PL(d_0)(dB) - 10 n \log\left(\frac{d}{d_0}\right) \quad (8)$$

where d_0 is 1km, $PL(d_0)$ is the 1km intercept point, and n is the path loss exponent. The results are presented in Table 1.

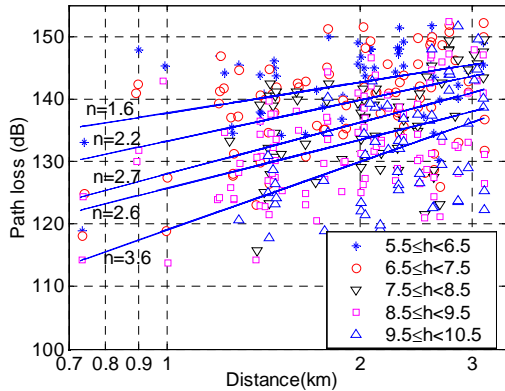


Figure 5. Path loss vs. distance and linear regression line fits for various SU antenna heights.

| SU height (m) | Path loss exponent (n) | 1km intercept (dB) | Standard deviation (dB) |
|---------------------|------------------------|--------------------|-------------------------|
| $5.5 \leq h < 6.5$ | 1.6 | 138 | 5.7 |
| $6.5 \leq h < 7.5$ | 2.2 | 133 | 6.9 |
| $7.5 \leq h < 8.5$ | 2.7 | 128 | 6.8 |
| $8.5 \leq h < 9.5$ | 2.6 | 126 | 7.1 |
| $9.5 \leq h < 10.5$ | 3.6 | 119 | 7.8 |

TABLE 1- Summary of path loss statistics for various SU antenna height.

| SU height (m) | Crosby (10) 2.4GHz | Crosby (10) 5.8GHz | Porter (3) 2.5GHz LOS | Porter (3) 2.5GHz NLOS |
|---------------|--------------------|--------------------|-----------------------|------------------------|
| 5 | 3.1 | 2.5 | 1.7 | 4.1 |
| 7.5 | 2.3 | 2.2 | - | - |
| 10.5 | 2.7 | 2.7 | 2.9 | 2.9 |

TABLE 2- Summary of path loss exponent for various SU antenna height due to (10) and (3).

The path loss exponent at 6m height is slightly less than the free space path loss exponent of 2. Path loss exponent values from previous studies by Crosby (10) and Porter (3) are presented in Table 2. It is reported in (3) that the path loss exponent decreases with increasing SU antenna height for non-line of sight (NLOS) cases. However because we do not distinguish the LOS cases from NLOS cases, it is difficult to compare our results with (3). Also note that at an SU antenna height of 5m, the path loss exponent of LOS cases in (3) is slightly less than the free space path loss exponent of 2, owing to limited data (3).

Similarly, the low path loss exponent we observed at an SU antenna height of 6m may be due to insufficient data recorded owing to the low signal to noise ratios in this highly shadowed region. In general the data that is successfully recorded will be at locations that experience less shadowing by nearby obstructions, thus giving an optimistic result.

Delay Spread Results

Figure 6 shows the cumulative distribution function of the RMS delay spread plotted for various SU antenna heights. The graph shows that RMS delay spreads at high SU antenna heights (9m and 10m) are significantly lower than those at low SU antenna heights. Table 3 summarises the RMS delay spread statistics. It shows that 90% of the RMS delay spread values are less than 100ns, except at an SU antenna height of 7m (130ns). However at lower SU antenna heights (6m, 7m, and 8m), the CDF plots of RMS delay spread are very close to each other, showing that the delay spread values at these heights are less distinguishable from each other, as is evident from their median values. The maximum delay spread also

decreases as the SU antenna height increases until the SU antenna height reaches 10m. Overall, the average RMS delay spread decreases with increasing SU antenna height.

This finding differs from (3) where it was found that the delay spread increased slightly with antenna height owing to the greater likelihood of the higher antenna gathering reflections from distant objects. Note that 90% of the RMS delay spread values reported in (3) are under 50ns. However because of the relatively few high rise building in our measurement area, this effect has not been observed. In fact, the RMS delay spread value is larger for lower SU antenna heights. This is due to the relatively stronger multipath components arriving at the SU, since the magnitude of the main path is diminished owing to increased shadowing in more NLOS conditions.

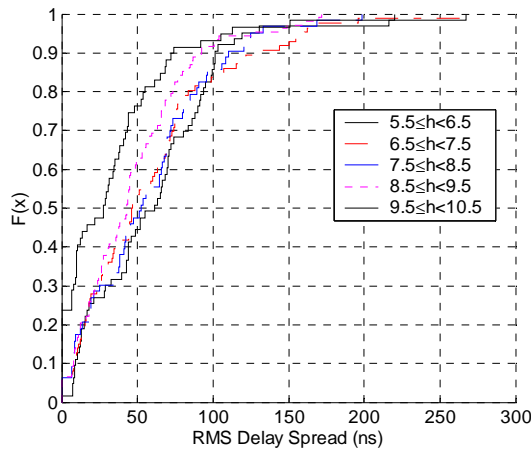


Figure 6. Cumulative distribution function of RMS delay spread for various SU antenna heights

| SU height (m) | Mean (ns) | Median (ns) | CDF 90% (ns) | Max Trms (ns) | Standard deviation (ns) |
|---------------|-----------|-------------|--------------|---------------|-------------------------|
| 5.5<h<6.5 | 61.4 | 61.4 | 101.4 | 267.5 | 47.9 |
| 6.5<h<7.5 | 58.6 | 46.4 | 129.6 | 266.4 | 50.6 |
| 7.5<h<8.5 | 56.6 | 52.3 | 109.9 | 198.5 | 42.7 |
| 8.5<h<9.5 | 47.3 | 43.1 | 89.4 | 172.1 | 37.6 |
| 9.5<h<10.5 | 34.3 | 27.8 | 73.8 | 220.5 | 40.7 |

TABLE 3- Summary of RMS delay spread for various SU antenna heights

Conclusions

This paper has shown the influence of SU antenna height on a BWA system employing directional SU antennas and sectorized BS antennas at 3.5 GHz. The path loss exponent at a SU antenna height of 10m is close to 4, and between 2.2 and 2.7 for SU antenna heights between 7m and 9m. The wideband characteristics of the BWA channel, as quantified by the RMS delay spread show that 90% of the channels

have a delay spread of less than 100ns. The average RMS delay spread is also observed to decrease with increasing SU antenna height. The maximum RMS delay spread observed in our measurements is less than 270ns.

References

- Cambridge Broadband Limited, 2001, "Single carrier and OFDM modulation: Their suitability for broadband fixed wireless access systems", <http://www.cambridgebroadband.com/>
- Crosby D., Greaves S. and Hopper A., 1999, "A Theoretical Analysis of Multiple Diffraction in Urban Environments for Wireless Local Loop Systems", Proceedings 9th Virginia Tech/MPRG Symposium on Wireless Personal Comms, Blacksburg, Virginia.
- Porter J. W., Thweatt J. A., 2000, "Microwave propagation characteristics in the MMDS frequency band", ICC2000 (International Conference on Communication) Conference Proceedings, 1578-1582.
- Gans M. J., Amitay N., Yeh Y. S., Damen T. C., Valenzuela R. A., Cheon C., Lee J., 2002, "Propagation Measurements for Fixed Wireless Loppes (FWL) in a Suburban Region With Foliage and Terrain Blockages", IEEE Trans. on Wireless Communications, Vol. 1, No. 2, 302-310.
- Erceg V., Michelson D. G., Ghassemzadeh S. S., Greenstein L. J., Rustako A. J., Guerlain P. B., Dennison M. K., Roman R. S., Barnickel D. J., Wang S. C., Miller R. R., 1999, "A Model for the Multipath Delay Profile of Fixed Wireless Channels", IEEE JSAC, Vol. 17, No. 3, 399-410.
- Siaud I., Morin B., 1999, "Investigation on radio propagation channel measurements at 2.2GHz and 3.5GHz for the fixed wireless access in an urban area" Ann. Telecommun., Vol 54, No. 9-10, 464-478.
- Bello P. A., 1963, "Characterization of Randomly Time-Variant Linear Channels", IEEE Trans on Communication Systems, Vol. CS-11, No. 1, 360-393
- Proakis, J. G., 1995, "Digital Communications", Third Edition, McGraw-Hill Book Company, New York, 68-72
- Cullen P. J., Fannin P. C., Molina A., 1993, "Wide-band Measurements and Analysis Techniques for the Mobile Radio Channel", IEEE Trans. On Vehicular Technology, Vol. 42, No. 4, 589-602.
- Crosby D., 2000, "Propagation Modelling for Directional Fixed Wireless Access Systems", PhD thesis, University of Cambridge.